JOC The Journal of Organic Chemistry

Article

pubs.acs.org/joc

Impact of Donor–Acceptor Functionalization on the Properties of Linearly π-Conjugated Oligomers: Establishing Quantitative Relationships for the Substituent and Substituent Cooperative Effect Based on Quantum Chemical Calculations

Elizabeth C. Varkey,[†,‡] Jürg Hutter,[‡] Peter A. Limacher,[§] and Hans P. Lüthi*[,†]

[†]Laboratory of Physical Chemistry, ETH Zurich, Zurich CH8093, Switzerland

[‡]Institute of Physical Chemistry, University of Zurich, Zurich CH8057, Switzerland

[§]Department of Chemistry & Chemical Biology, McMaster University, Hamilton, Ontario L8S 4L8, Canada

Supporting Information

ABSTRACT: To understand better the impact of donor–acceptor substitution on the properties of linearly π-conjugated compounds, we performed a computational study on a series of variably substituted trans-polyacetylenes, polyynes, and polythiophenes. The focus of this work is on how rapidly the impact of a given substituent or a given combination of substituents vanishes along the π-conjugated chain. The response of the structural (bond-length alternation, rotational barrier) and molecular properties ((hyper)polarizability, chemical shift) to substitution is analyzed using different protocols, including a superposition model for the evaluation of the cooperative effect of substituents in homo- and heterosubstituted oligomers. With the exception of the (hyper)polarizability, the impact of donor–acceptor substitution is found to vanish following an exponential. The rate of decay of the substituent impact is found to be characteristic for each backbone, whereas the choice of substituent determines the absolute value of the respective property. The combination of substituents is shown to determine whether the substituent cooperative effect on a property is of an enhancing or damping nature. The rate of decay of the cooperative effect on most properties, including the (hyper)polarizability, is also found to follow an exponential law.

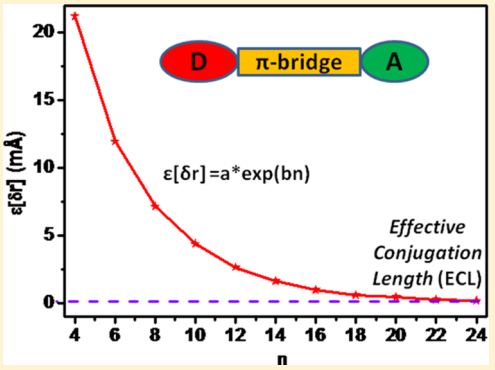

1. INTRODUCTION

It is well-known that the properties of π-conjugated polymers depend on the kind of chain (backbone), the number of repeating units (chain length), and on the type (donor, acceptor) and strength of the substituents. The fact that the molecular properties of these compounds respond very strongly to these parameters has led researchers to think about the laws that govern this context already at an early stage.[1−7] Concepts such as effective conjugation length (ECL),[8] confinement length (CL),[9] or delocalization length (DL),[9] which address the issues related to the saturation of a particular property with respect to the conjugation length, emerged. At the same time, quantitative structure–property relationships (QSPR) that model the dependence of molecular properties on chain size and substitution pattern were established.[3,8,10−22] In this context, Meier et al. were able to express the dependence of the longest wavelength of absorption (λ_{max}) on chain length for donor–acceptor-substituted polyacetylene.[3] These authors were able to show that for a given compound λ_{max} behaves exponentially with respect to the chain length, n, of the polyacetylene oligomer, allowing extrapolation to λ^{∞}_{max} as

$$\lambda_{(n)} = \lambda^{\infty}_{max} - (\lambda^{\infty}_{max} - \lambda_1)\, e^{-a(n-1)} \quad (1)$$

The growth functions proposed put forward the methodology to predict the ECL and the overall effect of conjugation with an increasing number of repeating units.[3] Recently, Tykwinski and co-workers successfully applied this approach to determine λ^{∞}_{max} of polyynes.[23]

For nonlinear optical properties such as the polarizability (α) and hyperpolarizability (γ),[3,14] Brédas et al. proposed a power law,[24,25] which describes the systematic increase of γ with respect to the extension of conjugation length. For small π-conjugated oligomers, the polarizabilities follow

$$y = an^b \quad (2)$$

where n stands for the number of repeating monomers and y is either alpha or gamma. For a larger oligomer size, the coefficient b will decrease toward unity, which indicates that the property grows linearly with respect to chain length.[24−27] At this point, it reaches the ECL.

Received: October 12, 2013
Published: November 25, 2013

In this article, we explore the impact of donor−acceptor substitution on the structural (bond-length alternation (BLA), barriers to rotation) and molecular properties ((hyper)-polarizability, chemical shift) of three different types of linear π-conjugated backbones (polyacetylene (PA), polyyne (PY), and polythiophene (PT); Scheme 1).

Scheme 1. Series of Extended π-Conjugated Oligomers (PA, PY, and PT with oligomer size $4 \leq n \leq 24$) Used in the Study

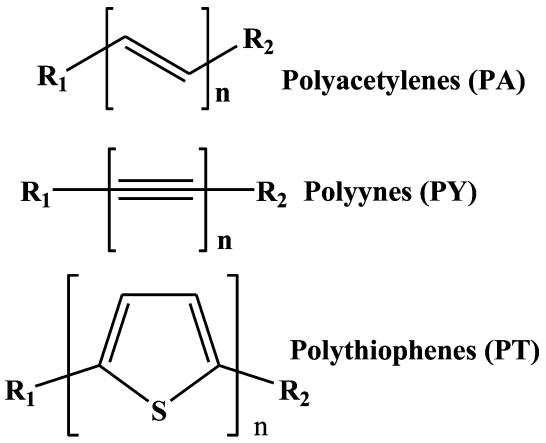

R_1, R_2 = H, NH_2, NO_2, CN & OH

In our studies, the chain length of the three oligomers is chosen to be sufficiently long so that the central carbon atoms will be free from the terminal substituent disturbances but short enough to show reasonably large substituent interactions. Trans-PA, PY, and PT chains with $4 \leq n \leq 24$ unsaturated bonds are used as the backbone, terminated on each side with either a π-electron-donor or π-electron-acceptor moiety, resulting in donor−acceptor (D−A), donor−donor (D−D), or acceptor−acceptor (A−A) substitution patterns. Our choice of substituents includes two electron-donor moieties ($-NH_2$ and $-OH$) and two electron-acceptor moieties ($-NO_2$ and $-CN$). In addition, unsubstituted ($-H$ moiety) as well as monosubstituted (D/A) molecules were evaluated.

In particular, we seek to find analytical expressions in the spirit of Meier et al. and Brédas et al.[3,8,10−15] describing the response of these properties to chain-length extension and the substitution pattern. These expressions will show the rate at which the substituent impact will vanish for a given type of backbone and how rapidly the ECL for that particular property will be reached. We also investigate the substituent cooperative effect on a property and its evolution with chain length using a simple protocol (superposition model) presented by the authors in refs 26 and 27 and others.[28] This model compares the properties computed for the real (P_{real}) doubly substituted ($R_1-\pi-R_2$) system with the properties computed for a virtual model compound (P_{model}) built by superposition of two singly substituted fragments according to

$$P_{model}(R_1-\pi-R_2) = P(R_1-\pi-H) + P(H-\pi-R_2) - P(H-\pi-H) \quad (3)$$

P_{model} can be considered as the value of the property for the noninteracting fragments, where $P(R_1-\pi-H)$ and $P(H-\pi-R_2)$ are the respective properties of the monosubstituted chain. (The contribution of the unsubstituted chain to the property needs to be subtracted to avoid double counting.) The contribution of the cooperative effect (q) on the properties is found by comparison of the real and model values as follows

$$q = (P_{real} - P_{model})/P_{model} \quad (4)$$

Whereas extrapolation laws can be used to predict the evolution of a property of a given functionalized compound, the superposition model gives an indication on how the interaction of the two substituents will affect (i.e., enhance or damp) this property.

The objective of this article is to understand better the impact of substituents on the properties of π-conjugated compounds and to establish quantitative structure−property relationships supporting the rational design of such systems. The focus is on the rate of decay of the substituent effect with increasing chain length and on the substituent cooperative effect emerging from different substitution patterns.

2. COMPUTATIONAL METHODS

The optimization of the equilibrium and transition-state structures was performed using the CAM-B3LYP[29]/6-31G* method as implemented in Gaussian 09.[30] For conjugated systems, this long-range corrected density functional, designed to overcome the overestimation of charge delocalization predicted by the Becke three-parameter exchange term,[31] was shown to give molecular structures very close to experimental findings.[32,33] The rotational barriers were evaluated on the basis of the internal rotation about the central single bond (i.e., the energy difference between the equilibrium geometry and the corresponding rotational transition-state geometry). The NMR chemical shifts were calculated by means of the gauge-independent atomic-orbital (GIAO) approximation[34,35] using the CAM-B3LYP/6-31G* method with tetramethyl silane (TMS) as the reference. The use of a larger basis set (aug-cc-pVDZ) does not have a significant impact on the trend observed.

The chemical shifts computed with the CAM-B3LYP functional compare well with earlier experimental and computed values reported for PY chains.[35−38] For PY with n = 16, the chemical shift we predict ranges between 56 and 65 ppm, which compares very well to the experimental value reported by Tykwinski (57−69 ppm).[38] Another computational study[35] using B3LYP/6-311G predicts slightly larger shifts (64−72 ppm) but a similar range (8 ppm). For PA, experimental results are available for the unsubstituted tetramer[39,40] and hexamer.[40] These agree well with the present computed values (experimental, 117−137 ppm versus calculated, 117−134 ppm for both n = 4 and 6). For PT, the agreement between experiment[41] and computation is not as good (experimental, 123−137 ppm versus calculated, 119−141 ppm), but we still expect the trends to be properly reproduced.

The longitudinal polarizability (α) and second hyperpolarizability (γ) were evaluated at the HF/6-31G* level, which was shown to be sufficiently accurate to reproduce correctly the evolution of these properties with chain length.[42−46] For every molecule, the longitudinal axis was defined as the principal axis with the lowest moment of inertia. The calculations of α and γ were performed using response theory as implemented in the Dalton quantum chemistry package.[47−49] The dipole moment and the first hyperpolarizabilty (β) were not explored because they both vanish for homopolar substitution (inversion symmetry).

The Cartesian coordinates of all three backbone types and for all substitution patterns (for n = 4) along with the input parameters used are given in the Supporting Information.

3. RESULTS AND DISCUSSION

3.1. Influence of Substituents on the Structural and Electronic Properties. As reported in a previous study,[27] the geometry of donor−acceptor-substituted polyacetylenes is not perfectly linear. For homopolar substitution patterns (donor−

donor, acceptor−acceptor), the polyacetylene backbone takes a slight S shape, whereas heteropolar (donor−acceptor) substitution results in a bow-shaped structure. Planarity, however, is always retained. These structural distortions are not observed for the polyyne and polythiophene backbones, which remain linear even for very long chains.

For local properties, such as the BLA, the barrier to rotation, or chemical shift, there are two ways to study the decay of the impact of terminal substituents along the π-conjugated chain: either one visits each bond or each atom along a sufficiently long backbone or one focuses on the center of the molecule and observes the development of the properties in response to chain-length extension. The latter approach, chosen in this work, has the advantage that local effects of the substituents can be screened more easily. For this matter, our observations always start with the tetramer (n = 4).

3.1.1. Central Bond-Length Alternation (δr). We observe a shortening of single bonds and elongation of double bonds (i.e., a reduction of the BLA) regardless of the substitution pattern (D−A, D−D, or A−A; Figure 1a). The effect decreases monotonically as we extend the length of the oligomer chain until it finally disappears (reaching the ECL) for this particular property. For the D−A-substituted oligomers, we also observe a convergence from lower to higher values of δr, whereas for the unsubstituted and the homosubstituted backbones, the convergence is from higher to lower values of δr. For all polyacetylene chains, δr converges to a value of 0.09 Å, whereas the polyyne and polythiophene analogues converge to a δr of 0.131 and 0.077 Å, respectively. The corresponding information is given in Supporting Information sections 2 and 3. The individual single- and double-bond lengths of substituted and unsubstituted PA (n = 20) are given in Supporting Information section 1.

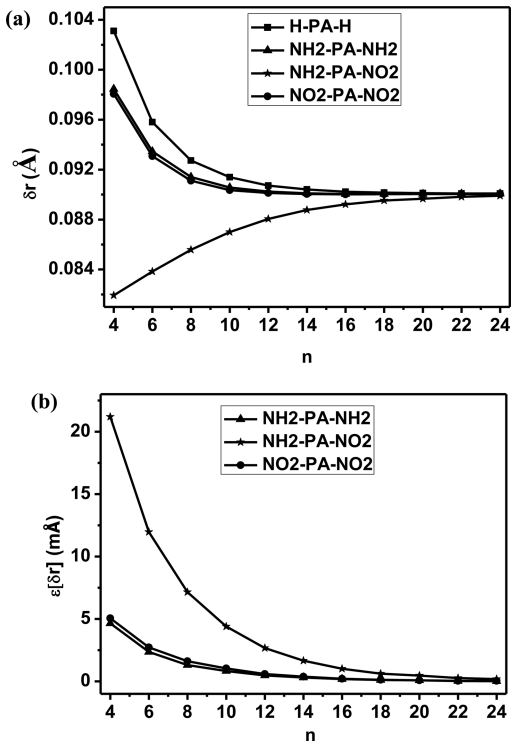

Figure 1. (a) Influence of different substitution patterns on the central BLA (δr in angstroms) on the polyacetylene backbone as a function of oligomer size. (b) Influence of different substitution patterns on $\varepsilon[\delta r]$ (eq 5).

Figure 1b compares the influence of terminal donor and acceptor (homo/hetero-) substitution on the central BLA as a function of chain length to the unsubstituted polyacetylene reference ($\varepsilon[\delta r]$). From Figure 1b, we clearly see that D−A substitution has more impact on the BLA than homopolar (D−D, A−A) substitution. Most notably, however, we see that the influence of the substituents drops systematically and at a constant rate for all substitution patterns.

Figure 2a,b shows the impact of substituents in terms of the difference between the central BLA of the unsubstituted

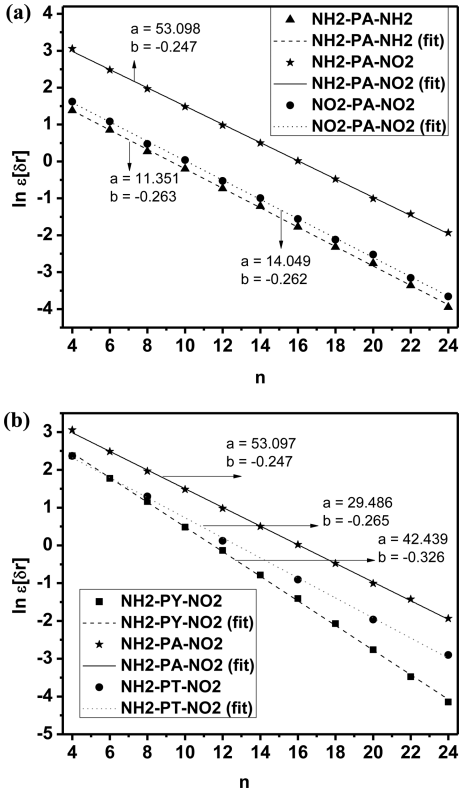

Figure 2. Influence of terminal substitution on the central BLA relative to the unsubstituted oligomer as function of (a) substitution pattern and (b) type of backbone. The graphs include the fits of ln $\varepsilon[\delta r]$ in units of milliangstroms as a function of oligomer size using the expression in eq 6.

reference and the substituted chain, $\varepsilon[\delta r]$, as a logarithmic plot. The mathematical form of $\varepsilon[\delta r]$ is given as

$$\varepsilon[\delta r] = \delta r(\mathrm{H}-\pi-\mathrm{H}) - \delta r(\mathrm{R}_1-\pi-\mathrm{R}_2) \quad (5)$$

The graphs show that the substituent impact on the central BLA decays according to an exponential law. Regardless of the kind of substitution pattern (Figure 2a) or backbone (Figure 2b), the graph of ln $\varepsilon[\delta r]$ as a function of chain length, to a good approximation, is a straight line.

The development of the substituent impact on $\varepsilon[\delta r]$ with respect to chain length n can therefore be expressed by means of the two-parameter analytical expression

$$\varepsilon[\delta r] = a^* \exp(bn) \quad (6)$$

for all backbones and all substitution patterns explored.

dx.doi.org/10.1021/jo4022869 | J. Org. Chem. 2013, 78, 12681−12689

Figure 2 shows that parameters a and b appear to be characteristic for the substitution pattern (D−A, D−D, and A−A) and for the type of backbone (PA, PY, and PT), respectively. From Figure 2a, we see that D−A substitution leads to the largest parameter value for parameter a, whereas from Figure 1b, we observe a slightly different slope (parameter b) for the three backbones with that particular substitution pattern. Figure 2a,b also shows that the quality of the fitting of $\varepsilon[\delta r]$ using the above expression is rather accurate (with a deviation of ±0.02 from the mean value). Note that the fits only start at chain length n = 4 to bypass terminal substituent disturbance.

Table 1 summarizes the values of a and b for all substitution patterns for PA. We see that parameter a is not only characteristic for the substitution pattern but also, to a lesser extent, for the substituent strength. For heteropolar substitution, we observe the highest values of a for the combination of strong substituents (NH_2−PA−NO_2; a = 53.1) and the lowest value for the combination of weaker substituents (OH−PA−CN; a = 23.7). Similar trends can be found for the homopolar and monosubstitution patterns. The same observation can also be made for PY and PT (see Supporting Information sections 4 and 5).

Table 1. Fitting Parameters for $\varepsilon[\delta r]$ Using the Analytical Expression $\varepsilon[\delta r] = a^* \exp(bn)$ for All Substitution Patterns of PA

$[\delta r]$	a	b	R^2
$\varepsilon[\delta r]$ H−PA−NH_2	13.363 (0.057)	−0.249 (0.004)	0.998
$\varepsilon[\delta r]$ NH_2−PA−CN	39.036 (0.050)	−0.241 (0.003)	0.998
$\varepsilon[\delta r]$ NH_2−PA−OH	11.599 (0.097)	−0.266 (0.006)	0.994
$\varepsilon[\delta r]$ NH_2−PA−NH_2	11.351(0.029)	−0.263 (0.002)	0.999
$\varepsilon[\delta r]$ NH_2−PA−NO_2	53.098 (0.025)	−0.247 (0.002)	0.999
$\varepsilon[\delta r]$ H−PA−NO_2	14.684 (0.030)	−0.233 (0.002)	0.999
$\varepsilon[\delta r]$ NO_2−PA−CN	13.433 (0.107)	−0.258 (0.008)	0.992
$\varepsilon[\delta r]$ NO_2−PA−NO2	14.049 (0.031)	−0.262 (0.002)	0.999
$\varepsilon[\delta r]$ NO_2−PA−OH	29.719 (0.043)	−0.241 (0.003)	0.999
$\varepsilon[\delta r]$ H−PA−CN	10.334 (0.108)	−0.241 (0.007)	0.992
$\varepsilon[\delta r]$ CN−PA−CN	13.246 (0.089)	−0.275 (0.006)	0.996
$\varepsilon[\delta r]$ CN−PA−OH	23.742 (0.052)	−0.25 (0.003)	0.998
$\varepsilon[\delta r]$ H−PA−OH	5.252 (0.122)	−0.277 (0.009)	0.991
$\varepsilon[\delta r]$ OH−PA−OH	6.937 (0.127)	−0.272(0.010)	0.992

Parameter b determines how rapidly the impact of the substituents for a given backbone vanishes and how fast the ECL for a property is reached. The chain length, n, at which a certain fraction, r, of the initial value of the property is reached is given by the expression $n = \ln(r)/b + 1$. For the different substitution patterns of PA where the value of b is found to vary between −0.277 H−PA−OH) and −0.233 (H−PA−NO_2; see Table 1), this means that the 10% threshold (r = 0.10) for the impact of the substitution on the BLA is reached at n = 12.3 and 13.9, respectively (relative to the value of $\varepsilon[\delta r]$ observed at n = 4). For PT and PY, this 10% threshold on average over all substitution patterns is reached earlier (n = 12.3 and 10.9), in line with the general perception that PA shows the largest conjugation efficiency.[50]

3.1.2. Central Barrier to Rotation (δE). A property closely related to the BLA is the barrier to rotation about the C−C single bonds. The more delocalized the charge, the shorter the single bonds, the higher their bond order and the larger the corresponding barrier to rotation. Given the fact that all substitution patterns lead to a reduction in the BLA, it is not surprising that the C−C barriers to rotation of the substituted PA and PT are consistently larger than the ones of the unsubstituted reference.

Figure 3a shows the barrier to rotation (δE) observed for different substitution patterns of PA as a function of oligomer size. δE is the energy difference between the equilibrium geometry and the twisted transition state. The δE values follow a similar pattern as δr. Except for the NH_2-substituted oligomers (not shown) the rotational barrier of all the substituted chains converges to the value observed for the unsubstituted compound (15.2 mH for PA, 4.89 mH for PT), indicating that the ECL for this property is reached within the range of chain lengths studied here. Because of a rehybridization of the N atom of the NH_2 group in the transition state, the NH_2 -substituted compounds converge to a different value for long chains. Figure 3b shows the impact of different substitution patterns on $\varepsilon[\delta E]$ (the difference between the central barrier to rotation of the substituted oligomers with the unsubstituted chain) (in mH). As for the BLA, a trend for the $\varepsilon[\delta E]$ was also observed, which can be expressed in terms of the analytical expression in eq 6. The average b of PT is found to be −0.308 (±0.05), which is higher than PA backbones (−0.285 with a deviation of ±0.04). This indicates the barrier to rotation of PT backbone reaches the ECL faster than PA. The graph showing curve fitting of the corresponding polymers is given in Supporting Information section 6.

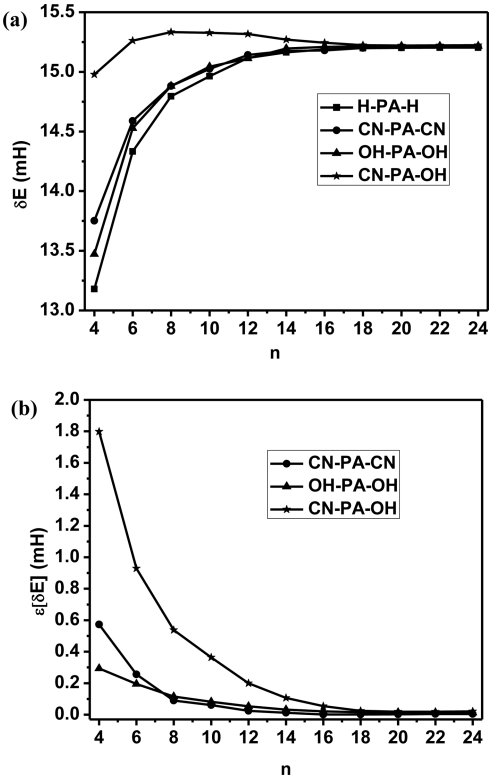

Figure 3. (a) Barrier to rotation (δE) in units of mH about the central single bond for different substitution patterns for the array of weaker substituents as a function of chain length. (b) Influence of different substitution patterns on $\varepsilon[\delta E]$ (the difference between the central barrier to rotation of the substituted oligomers with the unsubstituted chain) (in mH).

3.1.3. Polarizability and Hyperpolarizability. It is well-established that for short chain lengths the electronic

dx.doi.org/10.1021/jo4022869 | J. Org. Chem. 2013, 78, 12681−12689

contribution to the polarizability and hyperpolarizability can be expressed by means of the two-parameter law of the form $y = an^b$ (eq 2 presented in the Introduction). In a recent effort to understand the meaning of these two parameters,[26] we found that their interpretation is not as straightforward as for the (local) properties investigated here. We were able to demonstrate that there is an appreciable negative correlation between the exponent b and the logarithm of the pre-exponential factor a, $\ln(a)$: substitution patterns showing high values of b will generally show low values of the (hyper)-polarizability for short chains (and vice versa). Still, the highest values for the (hyper)polarizability are obtained with strong donor−acceptor-substitution patterns.

The (hyper)polarizability data presented here will be used to explore the cooperative effect of substituents. The computation of the hyperpolarizability of π-conjugated systems too large to be addressed by accurate methods (such as coupled cluster theory with an extended basis set) is still a difficult task. It was shown that the values obtained by Hartree−Fock theory tend to be more accurate than those obtained by density functional theory, even when long-range corrected exchange functionals are used.[42,51,52] The results obtained for the (hyper)-polarizability with various substitution patterns are given in Supporting Information sections 7−12.

3.1.4. Chemical Shift (δ). Various experimental and theoretical reports are available in the literature that study the NMR of short-chain polymers, especially the polyyne backbone with terminal substituents.[35−38] Recently, Tykwinski et al.[38] reported ^{13}C NMR chemical shifts of polyynes, confirming earlier observations of a specific pattern for the chemical shift along the oligomer chain. They, along with other authors, found oscillations in the chemical shift between the adjacent carbon atoms. Our calculations confirm this observation and also show that for an extended polymer these oscillations become less intense toward the center of the chain and that the chemical shift of even- and odd-numbered carbon atoms converge to the same value. This effect will be discussed in a forthcoming publication.

Figure 4a shows the trend for the chemical shift observed for different substitution patterns of the polyacetylene backbone as a function of chain length. δ represents the average of ^{13}C NMR chemical shifts of the central carbon atoms in even-numbered polyacetylene chains. The presence of acceptor groups results in deshielding (higher values of δ relative to H−PA−H). Similarly, the presence of donor groups causes shielding.

For homopolar substitution, the chemical shift of the two central carbons is identical. For heteropolar substitution, we have a shielding effect on one and a deshielding effect on the other atom, resulting in the cancellation of the averaged shift (Figure 4a). For the visualization of the substituent impact, it thus appears more appropriate to take the product of the differences between the substituted and the unsubstituted compound for each of the two central atoms:

$$\varepsilon[\delta] = (\delta_{\text{left}}(\text{H}-\pi-\text{H}) - \delta_{\text{left}}(\text{R}_1-\pi-\text{R}_2)) \times (\delta_{\text{right}}(\text{H}-\pi-\text{H}) - \delta_{\text{right}}(\text{R}_1-\pi-\text{R}_2)) \quad (7)$$

Figure 4b now shows the impact of donor−acceptor substitution more clearly. We also observe that the shielding and deshielding effects of the weaker acceptor and donor substituents are less strong. The analysis of chemical shift for PT shows a similar influence (Supporting Information sections 13 and 14), whereas the result for the PY series of compounds is puzzling: it appears that the product of chemical shifts according to eq 7 is positive. Evidently, in this case, the impact of the substituents cannot be explained in terms of the shielding and deshielding effects of the acceptor and donor substituents presented previously.

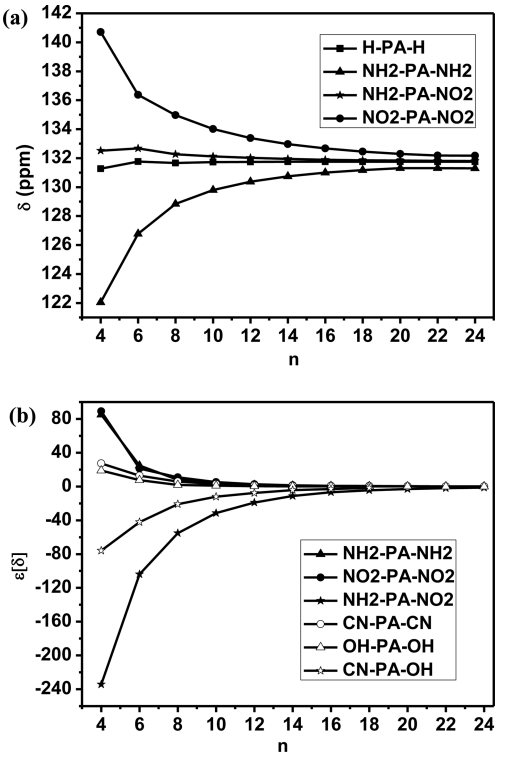

Figure 4. (a) Influence of different substitution patterns on the central ^{13}C NMR chemical shift (δ in ppm) of the substituted polyacetylene backbone as a function of chain length. (b) Influence of different substitution patterns and type of substituents on $\varepsilon[\delta]$ (in ppm).

However, as observed in properties such as δr and δE, we again find that the influence of the substituents on the chemical-shift ($\varepsilon[\delta]$) values drops exponentially and can again be expressed in terms of the analytical expression in eq 6. The average values of b (all substitution pattern) for PA, PY, and PT backbones are −0.207, −0.187, and −0.207, with the deviation from the mean of ±0.06, ±0.02, and ±0.03, respectively. The values of $\varepsilon[\delta]$ for the PY and PT backbones are given in Supporting Information sections 13 and 14.

3.2. Substituent Cooperative Effect on the Properties. In this work, we show along with other investigators[3,8,10−15,25] that the overall response of the properties of π-conjugated compounds to donor−acceptor substitution can be expressed by means of simple analytical expressions. In earlier work,[27] we also showed that part of the response of a given property can be ascribed to substituent cooperative effects (i.e., to the fact that a particular combination of substituents will have an effect on the property that is different from the sum of individual effect of the two substituents on this property). The application of the superposition model (eq 3) on the bond length of D−A-substituted polyacetylenes[26,27] showed that D−A substitution has an enhancing effect on electron delocalization, thus contributing to the reduction of BLA. Homopolar substitution, however, was shown to have the opposite effect (i.e., damping electron delocalization,thus increasing the BLA). In this section, we will further explore the cooperative effect of substituents to

dx.doi.org/10.1021/jo4022869 | J. Org. Chem. 2013, 78, 12681−12689

see whether the effect can be cast into similar analytical expressions as found for the overall substituent effect.

3.2.1. Cooperative Effect on Central BLA (δr) and Rotational Barrier (δE). Figure 5a,b presents the contribution

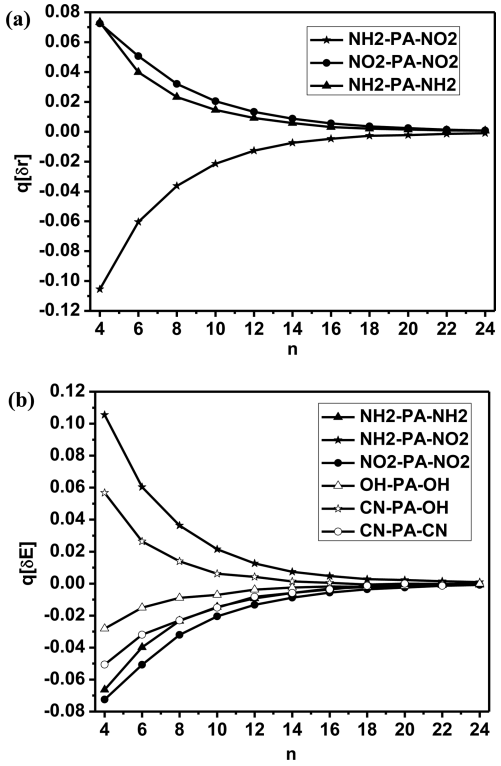

Figure 5. (a) Contribution of the cooperative effect of double substitution on the central BLA (δr) of the polyacetylenes as a function of oligomer size (n = 4–24). (b) Influence of terminal substitution on the cooperative effect of central rotational barrier (δE). Donor–acceptor-substituted polyacetylenes show an enhancing cooperative effect, whereas the homosubstituted polymers show a damping effect. The cooperative effect on the property decays exponentially toward zero for both the homo and hetero substitutions.

of cooperative effect on δr and δE as a function of chain length for the polyacetylene series. The quantity q is the contribution of cooperative effect, as defined in eq 4, where the sign and the magnitude of the effect for the properties depend on the substitution pattern and on the substituent strength. For δr, the homopolar substituent contribution to the respective properties is observed as positive and converges toward zero, whereas the heteropolar shows a negative contribution for the respective properties. The data for the cooperative effect of the other series can be found in Supporting Information sections 15 and 16. The important observation is that the superposition model reveals cooperative effects for all forms of conjugation. The cooperative effect for D–A conjugation on δr is always negative, thus enhancing electron delocalization that, in turn, leads to a reduced BLA, whereas an opposite trend is observed for both D–D and A–A conjugations.

The superposition model is also applied to the central rotational barrier of doubly (homo/hetero-) substituted oligomers. In Figure 5b, the cooperative effect on the rotational barrier of both strongly and weakly substituted oligomers is shown. For δE, the contribution of homopolar substituents is observed as negative and converges toward zero, whereas the heteropolar shows a positive convergence. As observed for the respective properties, the cooperative effect on δr and δE again follows a systematic decay, with D–A substitution showing an enhancing and D–D and A–A substitution showing a damping effect. In the graph, the cooperative effect is also shown for the polyacetylenes with weaker substituents. The cooperative effect on the rotational barrier for the polythiophenes was also analyzed, revealing similar damping (D–D and A–A) and enhancing (D–A) effects in response to donor and acceptor substitution.

The contribution of cooperative effect on both central bond-length alternation $q[\delta r]$ and central rotational barrier $q[\delta E]$ can be modeled by the analytical expression in eq 6. The graphs showing the contribution of cooperative effect on $q[\delta r]$ and $q[\delta E]$ of other polymers are given in Supporting Information sections 15–17.

3.2.2. Cooperative Effect on (Hyper)polarizabilities. We found a significant cooperative effect for the polarizability as well as for the second hyperpolarizability. According to the superposition model, the hyperpolarizability for the D/A system is enhanced by as much as 45% for small chains (Figure 6a,b). For the homopolar substitution, again, a damping effect on these two properties is observed. For both properties, the values of q converge toward zero in a systematic manner for all substitution patterns. The contribution of the cooperative effects on the (hyper)polarizabilities again follows the analytical expression in eq 6. The fitting parameters a and b are summarized in Table 2. Similar behavior is also observed for

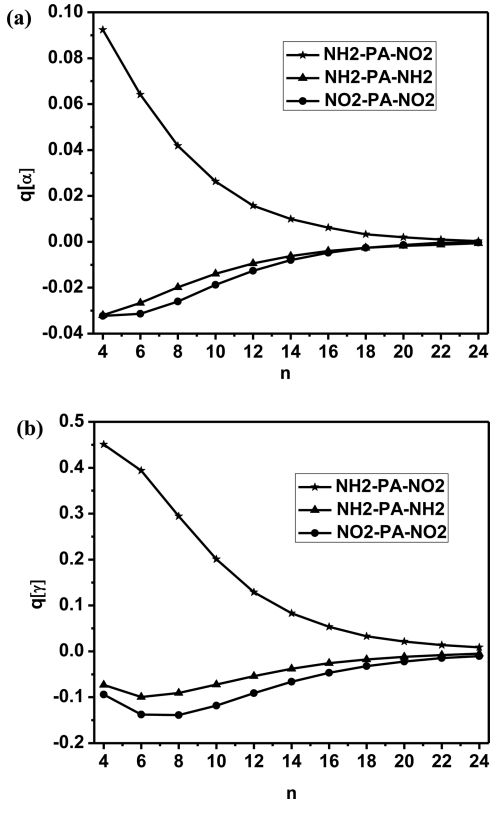

Figure 6. Contribution of the cooperative effect of terminal substitution on (a) polarizability (α) and (b) hyperpolarizability (γ) of homo- and heteropolar polyacetylene with $4 \leq n \leq 24$ chain length. Heteropolar polyacetylene shows an enhancing ($q > 0$) cooperative effect, whereas the homopolar oligomers show a damping effect ($q < 0$). An exponential trend for q toward zero for all substitution patterns is visible in both panels.

dx.doi.org/10.1021/jo4022869 | J. Org. Chem. 2013, 78, 12681–12689

Table 2. Fitting Parameters of q Based on the Expression $\ln(|q|) = \ln(a)+b*n$ for All Properties Showing a Cooperative Effect[a]

q	$\ln(a)$	b	R^2
$q[\delta r]$ NH_2–PA–NH_2	−1.826 (0.076)	−0.236 (0.005)	0.996
$q[\delta r]$ NH_2–PA–NO_2	−1.455 (0.094)	−0.236 (0.006)	0.993
$q[\delta r]$ NO_2–PA–NO_2	−1.646 (0.053)	−0.224 (0.003)	0.998
$q[\delta E]$ NH_2–PA–NH_2	−1.867 (0.066)	−0.234 (0.004)	0.997
$q[\delta E]$ NH_2–PA–NO_2	−1.455 (0.094)	−0.236 (0.006)	0.993
$q[\delta E]$ NO_2–PA–NO_2	−1.646 (0.053)	−0.224 (0.004)	0.998
$q[\alpha]$ NH_2–PA–NH_2	−2.336 (0.052)	−0.199 (0.004)	0.998
$q[\alpha]$ NH_2–PA–NO_2	−1.208 (0.090)	−0.251 (0.006)	0.994
$q[\alpha]$ NO2–PA–NO_2	−1.641 (0.127)	−0.235 (0.009)	0.992
$q[\gamma]$ NH_2–PA–NH_2	−0.799 (0.087)	−0.182 (0.005)	0.994
$q[\gamma]$ NH_2–PA–NO_2	−0.494 (0.053)	−0.216 (0.003)	0.998
$q[\gamma]$ NO_2–PA–NO_2	−0.277 (0.072)	−0.177 (0.004)	0.996

[a]For homopolar substitution the fit only starts with n = 8 (see also Figure 6).

Table 3. Average Value of Parameter b over All Substitution Patterns for a Given (Local) Property and a Given Backbone[a]

	b^{PA}	b^{PY}	b^{PT}	comments
$\varepsilon[\delta r]$	−0.256 ± 0.02	−0.334 ± 0.05	−0.277 ± 0.04	Table 1 and Figure 2a,b
$\varepsilon[\delta E]$	−0.285 ± 0.04		−0.308 ± 0.05	δE for PA (Supporting Information section 6) and PT
$\varepsilon[\alpha]$				not applicable, follows power law
$\varepsilon[\gamma]$				not applicable, follows power law
$\varepsilon[\delta]$	−0.207 ± 0.06	−0.187 ± 0.02	−0.207 ± 0.03	Figure 4b
$q[\delta r]$	−0.235 ± 0.02	−0.356 ± 0.04	−0.182 ± 0.04	Table 2 (PA only)
$q[\delta E]$	−0.231 ± 0.02		−0.393 ± 0.05	Table 2 (PA only)
$q[\alpha]$	−0.228 ± 0.04	−0.282 ± 0.01	−0.226 ± 0.04	Table 2 (PA only)
$q[\gamma]$	−0.192 ± 0.03	−0.217 ± 0.03	−0.207 ± 0.04	Table 2 (PA only)
$q[\delta]$				not applicable

[a]The list also includes the average value of b for the cooperative effect.

the weak–weak and strong–weak pairs for all other backbones (PY and PT; see sections 18–21 in the Supporting Information).

Mukamel and co-workers[28] investigated the cooperative effect (termed the intramolecluar charge-transfer effect) for the dipole, the polarizability, and the first hyperpolarizability of D–A-substituted PA and PY oligomers using the same superposition approach but with a fitting expression of the form $n^m \exp(bn)$. For the polarizabilities (α), a maximum of the effect is found for short D–A-substituted chains (n = 3 for PY and n = 6 for PA), after which the exponential behavior is domineering. Even though both studies use Hartree–Fock theory, we do not observe any maxima of the cooperative effects within the range of chain length studied (n > 3).

3.2.3. Cooperative Effect on the Chemical Shift. All structural and electronic properties discussed in the earlier sections show significant cooperative effects. However, in the case of the ^{13}C NMR chemical shifts, we notice only a marginal effect. The strongest cooperative effects are observed for the D–PA–A and A–PA–A oligomers. However, they only amount to +0.4 and −0.8%, respectively, which is found to be beyond the reliability of the superposition model.

4. OVERVIEW

We have seen that the (loss of) impact of homo- or heteropolar terminal substitution on the (local) properties of the three π-conjugated backbones explored in this work can be modeled by means of a two-parameter expression of the type $a* \exp(bn)$. The same expression can also be used to model the decay observed for the cooperative effects.

Table 3 gives an overview of the mean value of parameter b for all substitution patterns of all backbones and for all properties considered, including the respective cooperative effects. From the small deviation of b from the mean value, we see that for the local properties the parameter only moderately responds to the substitution pattern and therefore appears to be the characteristic for the backbone type (material constant). The same observation applies for parameter b in the context of the cooperative effect.

5. CONCLUSIONS

For all properties and for all backbones investigated, we find an exponential decay of the substituent impact with the increase in chain length n (i.e., with an increase of the distance to the substituent in the case of local properties). For the BLA, the rotational barrier, and the chemical shift, we find that the vanishing substituent impact can be modeled by a two-parameter law of the type $a* \exp(bn)$ regardless of the substitution pattern. For these properties, parameter b appears to be characteristic for the backbone (material constant) and only moderately responds to the substitution pattern. The pre-exponential factor a is found to be dependent on the type, strength, and combination of substituents.

Furthermore, the analysis of the substituent cooperative effect shows that it either has an enhancing (D–A) or damping (A–A and D–D) influence on the properties. This effect also follows an exponential behavior, even for the (hyper)-polarizability. However, no significant cooperative effect is observed for chemical shifts. Even if the reason for the observed exponential behavior is not yet understood, there is a known fact that the impact of a substituent or a substitution pattern

dx.doi.org/10.1021/jo4022869 | J. Org. Chem. 2013, 78, 12681–12689

follows a given law, which will be helpful for the rational design of π-conjugated materials.

■ ASSOCIATED CONTENT

Supporting Information

Effect of donor−acceptor substitution on the different backbones, including single- and double-bond lengths of substituted polyacetylene for oligomer size n = 20, δr as a function of chain length for the PY and PT backbones, $\varepsilon[\delta r]$ as a function of chain length for the PY and PT backbones, fit of $\varepsilon[\delta E]$ as a function of chain length for the PA backbone, polarizability as a function of chain length for all backbones, hyperpolarizability as a function of chain length for all backbones, $\varepsilon[\delta]$ of the PT and PY backbones as a function of chain length, contribution of the cooperative effect on central BLA of the PY and PT backbones, contribution of the cooperative effect on the central rotational barrier of the PT backbone, contribution of the cooperative effect on the polarizability of the PY and PT backbones, contribution of the cooperative effect on the hyperpolarizability of the PY and PT backbones, and Cartesian coordinates of all backbone types and all substitution patterns for n = 4. This material is available free of charge via the Internet at http://pubs.acs.org.

■ AUTHOR INFORMATION

Corresponding Author

*E-mail: luethi@ethz.ch.

Notes

The authors declare no competing financial interest.

■ ACKNOWLEDGMENTS

We are grateful to the Swiss Science Foundation and NSERC for financial support. We also thank Prof. Rik Tykwinski and Dr. Marc-Olivier Ebert for useful scientific discussions.

■ REFERENCES

(1) Kirtman, B. C. B. *Int. Rev. Phys. Chem.* **1997**, *16*, 389−420.
(2) Tykwinski, R. R.; Gubler, U.; Martin, R. E.; Diederich, F.; Bosshard, C.; Günter, P. *J. Phys. Chem. B* **1998**, *102*, 4451−4465.
(3) Meier, H. *Angew. Chem., Int. Ed.* **2005**, *44*, 2482−2506.
(4) Szafert, S.; Gladysz, J. A. *Chem. Rev.* **2006**, *106*, 1−33.
(5) Bunz, U. H. F. *Acc. Chem. Res.* **2001**, *34*, 998−1010.
(6) Cygan, M. T.; Dunbar, T. D.; Arnold, J. J.; Bumm, L. A.; Shedlock, N. F.; Burgin, T. P.; Jones, L., II; Allara, D. L.; Tour, J. M.; Weiss, P. S. *J. Am. Chem. Soc.* **1998**, *120*, 2721−2732.
(7) Donhauser, Z. J.; Mantooth, B. A.; Kelly, K. F.; Bumm, L. A.; Monnell, J. D.; Stapleton, J. J.; Price, D. W.; Rawlett, A. M.; Allara, D. L.; Tour, J. M. *Science* **2001**, *292*, 2303−2307.
(8) Meier, H.; Stalmach, U.; Kolshorn, H. *Acta Polym.* **2003**, *48*, 379−384.
(9) Zerbi, G.; Galbiati, E.; Gallazzi, M. C.; Castiglioni, C.; Del Zoppo, M.; Schenk, R.; Müllen, K. *J. Chem. Phys.* **1996**, *105*, 2509.
(10) Meier, H.; Gerold, J.; Jacob, D. *Tetrahedron Lett.* **2003**, *44*, 1915−1918.
(11) Meier, H.; Gerold, J.; Kolshorn, H.; Baumann, W.; Bletz, M. *Angew. Chem., Int. Ed.* **2002**, *41*, 292−295.
(12) Meier, H.; Gerold, J.; Kolshorn, H.; Mühling, B. *Chem.—Eur. J.* **2004**, *10*, 360−370.
(13) Meier, H.; Ickenroth, D. *Eur. J. Org. Chem.* **2002**, *2002*, 1745−1749.
(14) Meier, H.; Ickenroth, D.; Stalmach, U.; Koynov, K.; Bahtiar, A.; Bubeck, C. *Eur. J. Org. Chem.* **2001**, *2001*, 4431−4443.
(15) Meier, H.; Petermann, R.; Gerold, J. *Chem. Commun.* **1999**, 977−978.
(16) Lewis, G. N.; Calvin, M. *Chem. Rev.* **1939**, *25*, 273−328.
(17) Hirayama, K. *J. Am. Chem. Soc.* **1955**, *77*, 373−379.
(18) Hirayama, K. *J. Am. Chem. Soc.* **1955**, *77*, 379−381.
(19) Hirayama, K. *J. Am. Chem. Soc.* **1955**, *77*, 382−383.
(20) Hirayama, K. *J. Am. Chem. Soc.* **1955**, *77*, 383−384.
(21) Kuhn, H. *J. Chem. Phys.* **1948**, *16*, 840−841.
(22) Wenz, G.; Mueller, M. A.; Schmidt, M.; Wegner, G. *Macromolecules* **1984**, *17*, 837−850.
(23) Chalifoux, W.; Tykwinksi, R. *Nat. Chem.* **2010**, *2*, 967−971.
(24) Gubler, U.; Bosshard, C.; Günter, P.; Balakina, M. Y.; Cornil, J.; Brédas, J. L.; Martin, R. E.; Diederich, F. *Opt. Lett.* **1999**, *24*, 1599−1601.
(25) Brédas, J.; Adant, C.; Tackx, P.; Persoons, A.; Pierce, B. *Chem. Rev.* **1994**, *94*, 243−278.
(26) Borini, S.; Limacher, P. A.; Lüthi, H. P. *J. Chem. Phys.* **2009**, *131*, 124105-1−124105-10.
(27) Borini, S.; Limacher, P. A.; Lüthi, H. P. *J. Phys. Chem. A* **2010**, *114*, 2221−2229.
(28) Lee, J. Y.; Mhin, B. J.; Mukamel, S.; Kim, K. S. *J. Chem. Phys.* **2003**, *119*, 7519−7524.
(29) Yanai, T.; Tew, D. P.; Handy, N. C. *Chem. Phys. Lett.* **2004**, *393*, 51−57.
(30) Frisch, M. J.; Trucks, G. W.; Schlegel, H. B.; Scuseria, G. E.; Robb, M. A.; Cheeseman, J. R.; Scalmani, G.; Barone, V.; Mennucci, B.; Petersson, G. A.; Nakatsuji, H.; Caricato, M.; Li, X.; Hratchian, H. P.; Izmaylov, A. F.; Bloino, J.; Zheng, G.; Sonnenberg, J. L.; Hada, M.; Ehara, M.; Toyota, K.; Fukuda, R.; Hasegawa, J.; Ishida, M.; Nakajima, T.; Honda, Y.; Kitao, O.; Nakai, H.; Vreven, T.; Montgomery, Jr., J. A.; Peralta, J. E.; Ogliaro, F.; Bearpark, M.; Heyd, J. J.; Brothers, E.; Kudin, K. N.; Staroverov, V. N.; Kobayashi, R.; Normand, J.; Raghavachari, K.; Rendell, A.; Burant, J. C.; Iyengar, S. S.; Tomasi, J.; Cossi, M.; Rega, N.; Millam, J. M.; Klene, M.; Knox, J. E.; Cross, J. B.; Bakken, V.; Adamo, C.; Jaramillo, J.; Gomperts, R.; Stratmann, R. E.; Yazyev, O.; Austin, A. J.; Cammi, R.; Pomelli, C.; Ochterski, J. W.; Martin, R. L.; Morokuma, K.; Zakrzewski, V. G.; Voth, G. A.; Salvador, P.; Dannenberg, J. J.; Dapprich, S.; Daniels, A. D.; Farkas, Ö.; Foresman, J. B.; Ortiz, J. V.; Cioslowski, J.; Fox, D. J. *Gaussian 09*, revision A.1; Gaussian, Inc.: Wallingford, CT, 2009.
(31) Becke, A. D. *J. Chem. Phys.* **1993**, *98*, 5648−5652.
(32) Limacher, P. A.; Mikkelsen, K. V.; Lüthi, H. P. *J. Chem. Phys.* **2009**, *130*, 194114.
(33) Peach, M. J. G.; Tellgren, E. I.; Sałek, P.; Helgaker, T.; Tozer, D. J. *J. Phys. Chem. A* **2007**, *111*, 11930−11935.
(34) Wolinski, K.; H. J., F.; Pulay, P. *J. Am. Chem. Soc.* **1990**, *112*, 8251−8260.
(35) Mahbubul Haque, M.; Yin, L.; Nugraha, A. R. T.; Saito, R. *Carbon* **2011**, *49*, 3340−3345.
(36) Wakabayashi, T.; Tabata, H.; Doi, T.; Nagayama, H.; Okuda, K.; Umeda, R.; Hisaki, I.; Sonoda, M.; Tobe, Y.; Minematsu, T.; Hashimoto, K.; Hayashi, S. *Chem. Phys. Lett.* **2007**, *433*, 296−300.
(37) Shindo, F.; Bènilan, Y.; Chaquin, P.; Guillemin, J. C.; Jolly, A.; Raulin, F. *J. Mol. Spectrosc.* **2001**, *210*, 191−195.
(38) Tykwinski, R. R.; Luu, T. *Synthesis* **2012**, *44*, 1915−1922.
(39) Spangler, C. W.; Little, D. A. *J. Chem. Soc., Perkin Trans. 1* **1982**, 2379−2385.
(40) Block, E. A. M.; Eswarakrishnan, V.; Gebreyes, K.; Hutchinson, J.; Iyer, R.; Laffitte, J.-A.; Wall, A. *J. Am. Chem. Soc.* **1986**, *108*, 4568−4580.
(41) Meyer, A. S. E.; Luppertz, F.; Schnakenburg, G.; Gadaczek, I.; Bredow, T.; Jester, S.-S.; Höger, S. *Beilstein J. Org. Chem.* **2010**, *6*, 1180−1187.
(42) Limacher, P. A.; Li, Q.; Lüthi, H. P. *J. Chem. Phys.* **2011**, *135*, 014111-1−014111-4.
(43) Wouters, S.; Limacher, P. A.; Van Neck, D.; Ayers, P. W. *J. Chem. Phys.* **2012**, *136*, 134110-1−134110-13.
(44) Dixit, S. N.; Guo, D.; Mazumdar, S. *Phys. Rev. B.* **1991**, *43*, 6781−6784.
(45) Meyers, F.; Brédas, J. L.; Zyss, J. *J. Am. Chem. Soc.* **1992**, *114*, 2914−2921.
(46) Shuai, Z.; Brédas, J. L. *Phys. Rev. B.* **1991**, *44*, 5962−5965.

(47) Helgaker, T.; Coriani, S.; Jörgensen, P.; Kristensen, K.; Olsen, J.; Ruud, K. *Chem. Rev.* **2012**, *112*, 543−631.
(48) *DALTON*, a molecular electronic structure program, release 2.0, 2005; http://www.kjemi.uio.no/software/dalton/dalton.html.
(49) Jansik, B.; Salek, P.; Jonsson, D.; Vahtras, O.; Agren, H. *J. Chem. Phys.* **2005**, *122*, 054107-1−054107-19.
(50) Bruschi, M.; Limacher, P. A.; Hutter, J.; Lüthi, H. P. *J. Chem. Theory Comput.* **2009**, *5*, 506−514.
(51) Song, J.-W.; Watson, M. A.; Sekino, H.; Hirao, K. *Int. J. Quantum Chem.* **2009**, *109*, 2012−2022.
(52) Champagne, B.; Kirtman, B. *Int. J. Quantum Chem.* **2009**, *109*, 3103−3111.